Selective Medical Image Compression using Wavelet Techniques*

Alfred Bruckmann and Andreas Uhl

RIST++ (Research Institute for Softwaretechnology), University of Salzburg

Selective Image Compression (SeLIC) is a compression technique where explicitly defined regions of interest (RoI) are compressed in a lossless way whereas image regions containing unimportant information are compressed in a lossy manner. Such techniques are of great interest in telemedicine or medical imaging applications with large storage requirements. In this paper we introduce and compare different techniques based on wavelet transforms and demonstrate their good performance which is mainly due to the spatial locality of the wavelet transform domain.

Keywords: wavelet image compression, region of interest coding, selective image compression

1. Introduction

Wavelet-based image processing methods have gained much attention in the biomedical imaging community. Applications range from pure biomedical image processing techniques such as noise reduction, image enhancement, and detection of microcalcifications in mammograms to computed tomography (CT), magnetic resonance imaging (MRI), and functional image analysis (positron emission tomography (PET) and functional MRI) [35, 1].

Image compression methods that use wavelet transforms (which are based on multiresolution analysis – MRA) have been successful in providing high rates of compression while maintaining good image quality, and have proven to be serious competitors to discrete cosine transform-(DCT) [38] or fractal-[11] based compression schemes. Panych [23] and Urriza [36] discuss aspects of wavelet-based compression of medical images, wavelet-based compression of medical video data is described by Ho [15] and Wang [39].

Medical image compression is constrained by the fact that most radiologists are not willing to base a diagnosis on an image that has been compressed in a lossy way. This is partially due to legal reasons (depending on the corresponding country's laws) and partially due to the fear of misdiagnosis because of lost data in the compression procedure [40]. Therefore, only lossless techniques are accepted, which limits the amount of compression to a factor of about 3 (in contrast to factors of 100 or more achievable in lossy schemes). On the other hand, many medical professionals are convinced that the future of health care will be shaped by technologies such as telemedicine. Applications of this type demand lower data rates as are achievable with lossless schemes [7]. This shows the need for efficient and widely accepted techniques for medical image compression.

This paper presents methods based on wavelet techniques for the compression of medical images that allow an image to be selectively compressed. Parts of the image that contain crucial information (regions of interest (RoI), e.g. microcalcifications in mammograms) are compressed in a lossless way whereas regions containing unimportant information are compressed in a lossy manner. This leads to considerably higher compression rates as compared to pure lossless schemes while critical information is preserved.

* This work was partially supported by the Austrian Science Fund FWF, project no. P11045-ÖMA and has been awarded a prize for medically relevant basic research of the Faculty for Natural Sciences, Univ. Salzburg, the so-called "Sackler-Award".

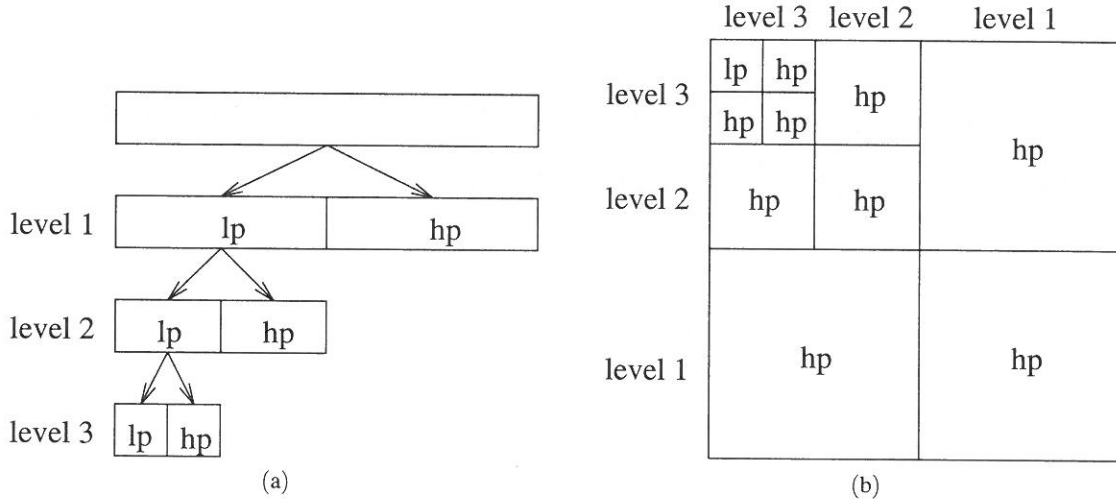

Fig. 1. 1-D and 2-D wavelet decomposition: lowpass (lp) and highpass (hp) subbands, decomposition levels (level 1 – level 3).

In block-based image compression schemes selective image compression (SeLIC) techniques may be applied in a straightforward way – blocks containing RoI are compressed in a lossless mode, and the remaining blocks in a lossy manner (for a SeLIC scheme based on fractal compression see Sheppard [28]). In contrast to such compression schemes, wavelet compression is applied to the entire image. Although at first sight this seems to be a disadvantage for wavelet-based SeLIC techniques, it turns out to allow very efficient SeLIC schemes, a fact which is mostly due to the spatial locality of the wavelet transform domain.

2. Wavelet Image Compression

A wide variety of wavelet-based image compression schemes have been reported in the literature [3, 14, 19], ranging from simple entropy coding to more complex techniques such as vector quantization [2, 8], adaptive transforms [10, 33], zero-tree encoding [26], and edge-based coding [12]. The latest compression algorithms are based on set partitioning in hierarchical trees [25] and some improvements in arithmetic coding [41]. In most of these schemes, compression is accomplished by applying a fast wavelet transform to decorrelate the image data, quantizing the resulting transform coefficients (this is where the actual lossy compression takes place) and coding the quantized values taking into account the high inter-subband correlations.

The fast wavelet transform (which is used in signal and image processing) can be efficiently implemented by a pair of appropriately designed Quadrature Mirror Filters (QMF). Therefore, wavelet-based image compression can be viewed as a form of subband coding. A 1-D wavelet transform of a signal s is performed by convolving s with both QMF's and downsampling by 2; since s is finite, one must make some choice about what values to pad the extensions with [31]. This operation decomposes the original signal into two frequency bands (called subbands), which are often denoted as coarse scale approximation (lowpass subband) and detail signal (highpass subband). Then, the same procedure is applied recursively to the coarse scale approximations several times (see Figure 1.a).

The classical 2-D transform is performed by two separate 1-D transforms along the rows and the columns of the image data, resulting at each decomposition step in a low pass image (the coarse scale approximation) and three detail images (see Figure 1.b); for more details see Mallat [20].

The techniques described in the next section may be applied to all compression schemes us-

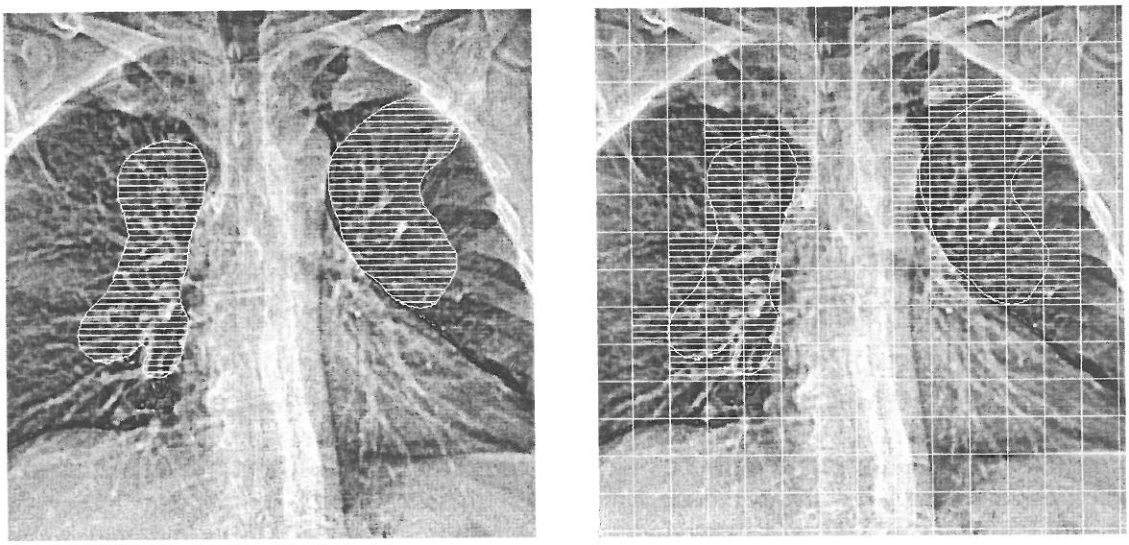

(a) (b)

Fig. 2. Block-based and arbitrarily-shaped RoI.

ing a scalar quantization procedure with subsequent entropy coding including the most efficient and recent ones [26, 25, 41]. If vector quantization [8] is to be used, SeLIC is restricted to the block-based approach.

3. Selective Wavelet Medical Image Compression

In this work we do not cover the question as to how RoI may be determined automatically (e.g., this could be achieved using wavelet techniques again for the detection of microcalcifications in mammograms [30]). We assume that RoI are determined interactively by marking these (arbitrarily shaped) regions on the screen, usually by an expert (radiologist). We have developed a graphical user interface which allows such interactive marking of RoI.

All types of algorithms described in Sections 3.1 and 3.2 allow the selection of arbitrarily-shaped RoI. In the block-based approaches (Section 3.1) the selected RoI are approximated by a set of square blocks. Therefore, image data not contained in the RoI are coded in lossless mode due to additional boder data caused by the approximation error. In the non block-based methods (Section 3.2 – "generic wavelet approaches") only image data belonging to the RoI are coded in lossless mode via the information of the importance map (see Figure 2 for the representation of these techniques in the graphical user interface).

Previous work on compressing different regions in an image with different rates has been performed by Jawerth [17] – in this early work the interaction between lossless and lossy schemes, details on quantization aspects, and the actual image coding are not discussed. Emphasis is given to the theoretical investigation of assigning different weights to coefficients in the transform domain.

It should be noted that the algorithms introduced are composed of entirely independent components (i.e. lossless coding, lossy wavelet coding, and shape coding of the RoI) resulting in a modular structure. Only in a concrete implementation it is determined which technique is used for which component of the algorithms (e.g., the lossless compression of the RoI may be performed using any type of lossless coding including runlength, Huffman, arithmetic, Lempel-Ziv, lossless predictive, or arithmetic coding).

3.1. Block-based Techniques

The image data to be compressed consist of two types of blocks (typically of size 32×32). The

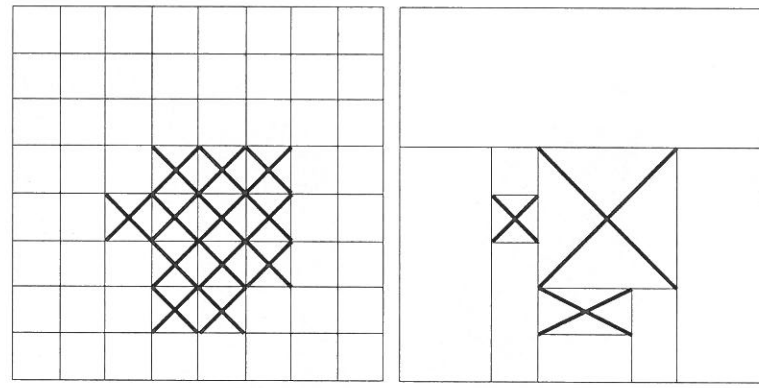

Fig. 3. Algorithms 1 and 2: marked regions are covered with the lossless mode.

first type is compressed in a lossless mode. The second type is compressed in a lossy mode with the wavelet coder. This leads us immediately to the question of how to compress image subblocks with a wavelet coder.

Significant work has already been done covering related topics, ranging from discussions concerning border treatment in wavelet transforms [31] to the construction of interval-based wavelet transforms and algorithms [6, 21]. Moreover, block-based wavelet image compression schemes have been investigated extensively using fixed image tilings [4, 16], adaptive image tilings [32], and the "Double Tree Algorithm" [13, 24].

We propose the following algorithms:

- **Algorithm 1**: The blocks not to be coded in lossless mode are compressed lossy with the wavelet coder (unmarked blocks in Figure 3 left) which
  - **1a** uses a classical wavelet transform with periodic padding at the edges of the image.
  - **1b** uses a classical wavelet transform with cutoff at the edges of the image.
  - **1c** uses a classical wavelet transform with mirroring at the edges of the image.
  - **1d** uses an interval-based wavelet transform with especially designed border filters [6].
  - **s1x** uses one of the techniques mentioned above and subsequent smoothing of the borders of the image blocks (e.g., Algorithm s1a consists of applying Algorithm 1a with subsequent smoothing operation).
- **Algorithm 2**: Usually, wavelet algorithms achieve better results for larger blocks (block border effects and the amount of side information increase for smaller blocks). Therefore we recombine all blocks which are to be compressed in lossy mode to larger blocks instead of applying the wavelet coder to each small block separately (see Figure 3 right). Similarly, instead of compressing the RoI on a block-by-block basis as in Algorithm 1, the RoI blocks are recombined as well prior to the lossless coding procedure. In analogy to Algorithms 1 we may again distinguish among Algorithms 2a – 2d and Algorithms s2a – s2d.

3.2. Generic Wavelet Techniques

The image data to be compressed consist of different components (as in the previous section): the RoI and the remainder. The RoI data consist of one or more arbitrarily-shaped parts of the image to be compressed in lossless mode; the remainder (again with arbitrary shape) is to be compressed in a lossy mode. The RoI data consist of two parts – the actual image data (gray values, texture information) and information about the shape and position of the region. Shape and position are represented by a binary image consisting of 0's (for already lossless compressed regions) and 1's (for the remainder). We denote this binary image as "importance map". In the emerging MPEG-4 standard a similar concept for coding shape and position of objects in different video object planes (VOPs) is denoted as "alpha plane" concept [29].

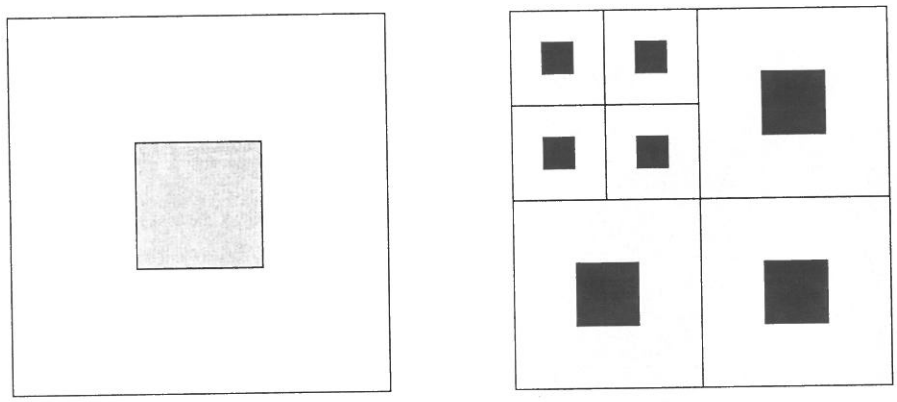

Fig. 4. RoI (gray region on the left side) and corresponding wavelet domain importance map (right side).

- **Algorithm 3**: After having compressed the RoI, the region is

  3a either left in the image where it was

  3b or subtracted from the image and replaced by a region consisting of pixels with uniform gray-value.

  Subsequently the resulting image is compressed using a regular wavelet coder (which is applied to the entire image); therefore, the RoI data are partially coded twice.

- **Algorithm 4**: The remainder of the image is compressed in a lossy manner by applying a wavelet transform to the entire image.

  The importance map is projected into the wavelet domain (see Figure 4). The wavelet domain importance map determines the wavelet coefficients which belong to the remainder of the image. This side information is used in the quantizer and coder step – these operations are performed taking into account which part of the data belongs to the remainder on a coefficient-by-coefficient basis. Coefficients with a 0 at the corresponding position of the wavelet domain importance map are simply discarded.

  The possibility of performing this operation on a coefficient-by-coefficient basis is due to the spatial locality of the wavelet transform domain. This technique is not possible using, e.g., a Fourier or DCT approach where only global frequency information is available.

4. Experimental Results

The following components are used for the algorithms in our experiments:

- **Lossless coding**: we apply a 2-D adaptive linear prediction with subsequent Huffman error coding (similar to [18]). Other possible choices are described by Nijim [22] and Shen [27].

- **Lossy wavelet coding**: we use Daubechies' compactly-supported wavelets [9] with 10 filter taps (we successfully used the corresponding family of filters in our previous work [33, 34], see Villasenor [37] for a discussion about proper filter choice for wavelet coding) and maximal decomposition depth (depending on image or block size). The lowpass approximation is coded in lossless mode, whereas highpass subbands are adaptively scalar-quantized using a variance-based bit allocation procedure. The quantized coefficients are coded by employing a combination of Huffman and runlength coding (similar to the JPEG algorithm).

- **RoI shape/position coding**: the importance map is compressed using a technique derived from facsimile compression (a variant of runlength coding combined with an XOR operation). This and other possiblities are investigated within the MPEG-4 standardization process [29].

We have chosen relatively large RoI in order to present results of borderline applications – if smaller RoI are considered, the achievable

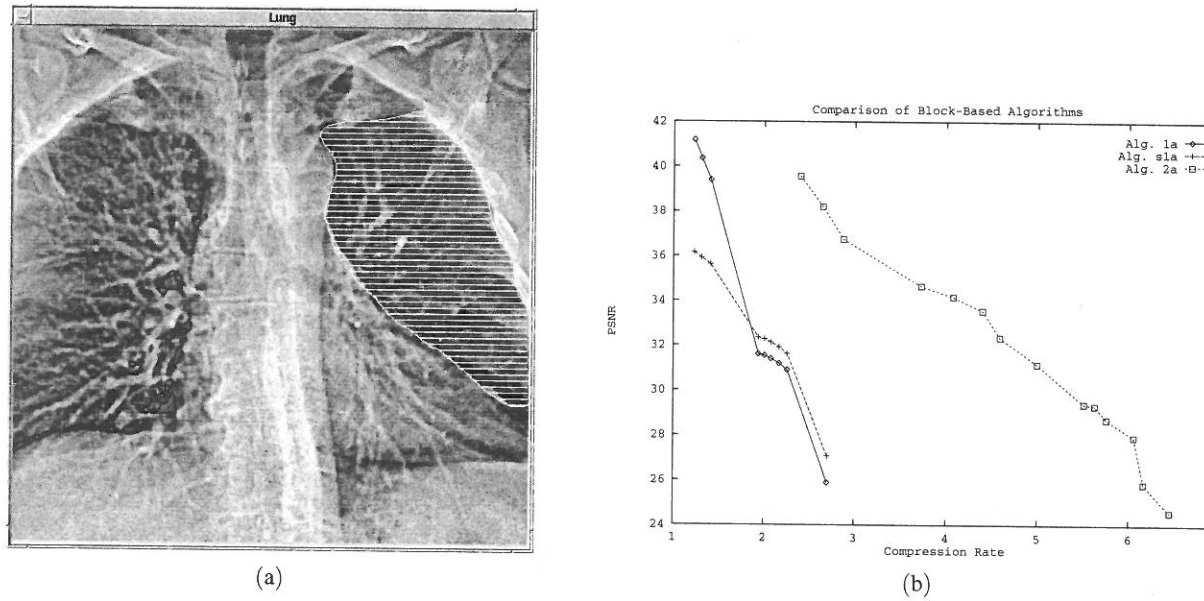

(a) (b)

Fig. 5. Test image (8bpp, 512 × 512 pixels Lung CT) with one RoI within the graphical user interface (a) and corresponding rate/distortion performance for Algorithms 1 and 2 (b).

compression rates are much higher. (Considering a RoI which covers 20% of the entire image and a maximal lossless compression rate for this region of 2.5, we obtain an upper bound compression rate of 12.5 for the entire image; this bound may only be reached if no data of the "unimportant" regions are stored.)

The compression rate is defined as

$$\frac{\text{number of bits in the original image}}{\text{number of bits in the compressed image}}.$$

Peak signal-to-noise ratio (PSNR) is used as an objective measure of image quality and is defined as follows (measured in deciBel dB):

$$PSNR = 10 \log_{10} \frac{255^2}{e_{ms}^2}$$

where 255 is the maximal gray-value of the original image and e_{ms}^2 is the average sample mean-squared error.

$$e_{ms}^2 = \frac{1}{N^2} \sum_{i=1}^{N} \sum_{j=1}^{N} (f(i,j) - \hat{f}(i,j))^2$$

where $f(i,j)$ and $\hat{f}(i,j)$ represent the $N \times N$ original and the reproduced images, respectively. The data of the compressed image obviously consist of both the lossless and lossy coded parts, plus the necessary side information (e.g. in which way particular blocks are coded or the importance map in the generic wavelet case).

We use three test images with 8 bits/pixel (bpp) and 512 × 512 pixels each. Figure 5.a shows a Lung CT with one large RoI, Figure 5.b displays a comparison of Algorithms 1a, s1a and 2a for this image. The superior performance of Algorithm 2a is clearly exhibited. Also, we note the better behavior of the algorithm with block smoothing, which is even more pronounced by visual inspection (see Figure 6). The same effect may be observed in even stronger fashion for the digital angiogram (with two RoI, see Figure 7.a) in Figure 7.b, where we notice a PSNR gain of up to 3.5 dB for compression rates above 2. These observations hold for all smoothing techniques. Concerning the variants a – d in Algorithms 1 and 2, there is a clear ranking: cutoff performs worst, interval filters best, and periodizing and mirroring perform almost equally between the two former modes.

The effect of different block sizes in Algorithms 1 and 2 is documented in Figure 8.a. We observe increasing image quality along with increasing block sizes. These results are due to the large amount of side information and poor performance of the wavelet coder for small block

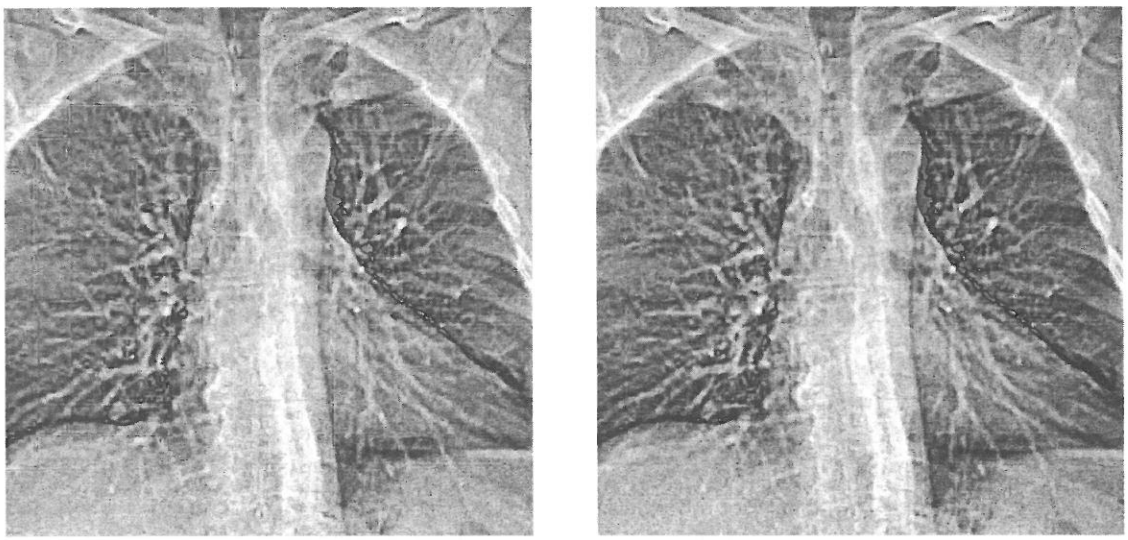

(a) (b)

Fig. 6. Comparison of algorithms 1a and s1a: without (a) and with block smoothing (b) (for RoI in Figure 5.a).

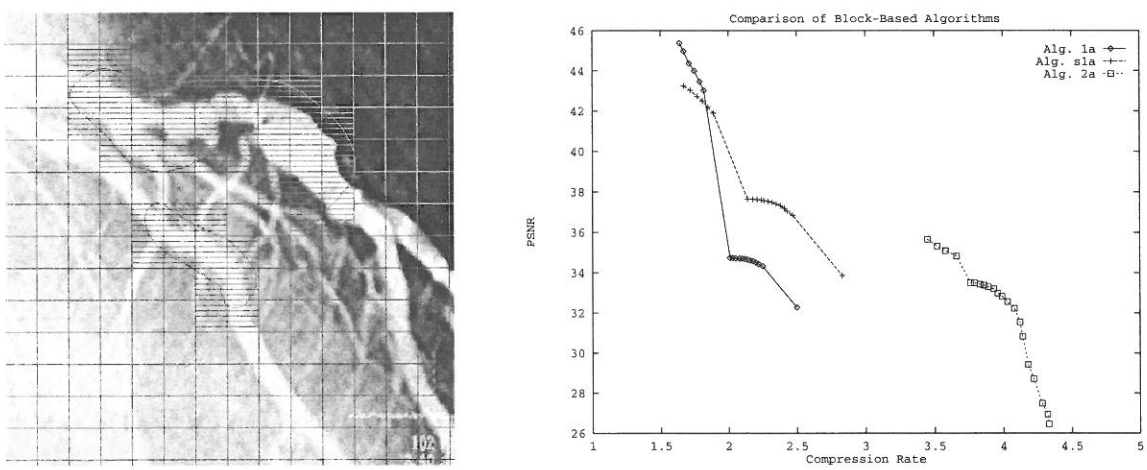

(a) (b)

Fig. 7. Digital angiography (8bpp, 512 × 512 pixels) with RoI (a) and corresponding rate/distortion performance for Algorithms 1a (with and without smoothing) and 2a (b).

sizes. Of course, this effect is limited at block size 32, because at size 64 too much image information outside the RoI is coded in lossless mode to achieve competitive results. Additionally, these results depend strongly upon the shape of the RoI.

Figure 8.b shows a comparison among Algorithms 3a, 3b, and 4. Algorithm 4 gives the best results (as we expect), whereas it is somehow surprising that Algorithm 3a outperforms 3b. This is probably due to the discontinuities in the transform domain introduced by Algorithm 3b.

Finally, we compare the performance of Algorithms 2a and 4 (i.e. the best block-based and the best generic algorithms). Figure 9 compares the effects if two differently structured RoI are chosen within the same image. Whereas Figure 9.a displays the rate/distortion performance for one large RoIs (compare Figure 5.a), Figure 9.b documents the same measurements for two smaller RoIs (compare Figure 2). The superior

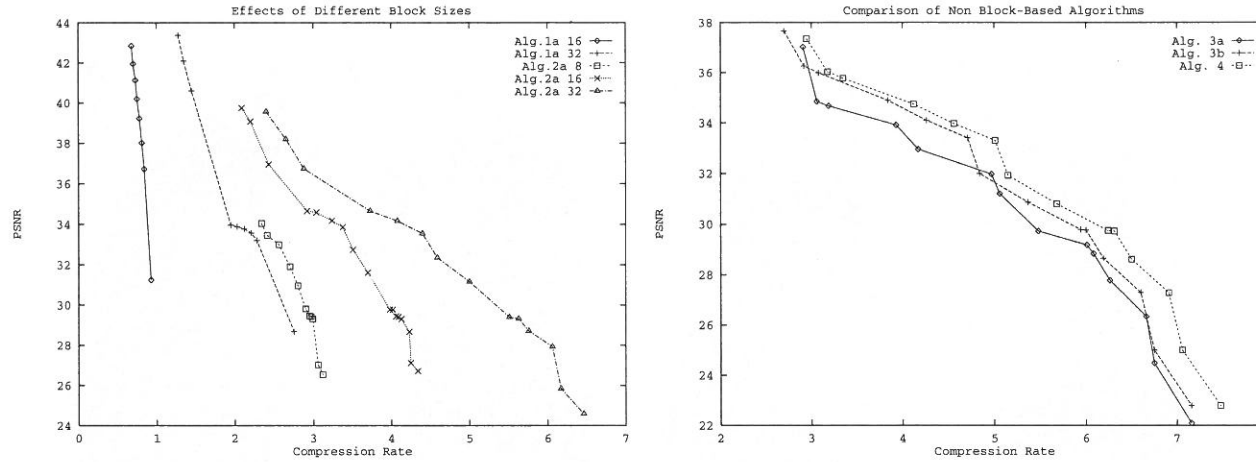

Fig. 8. Rate/distortion performance for different block-sizes in Algorithms 1a and 2a (a) and comparison of Algorithms 3 and 4 (b) (applied to the image and RoI in Figure 5.a).

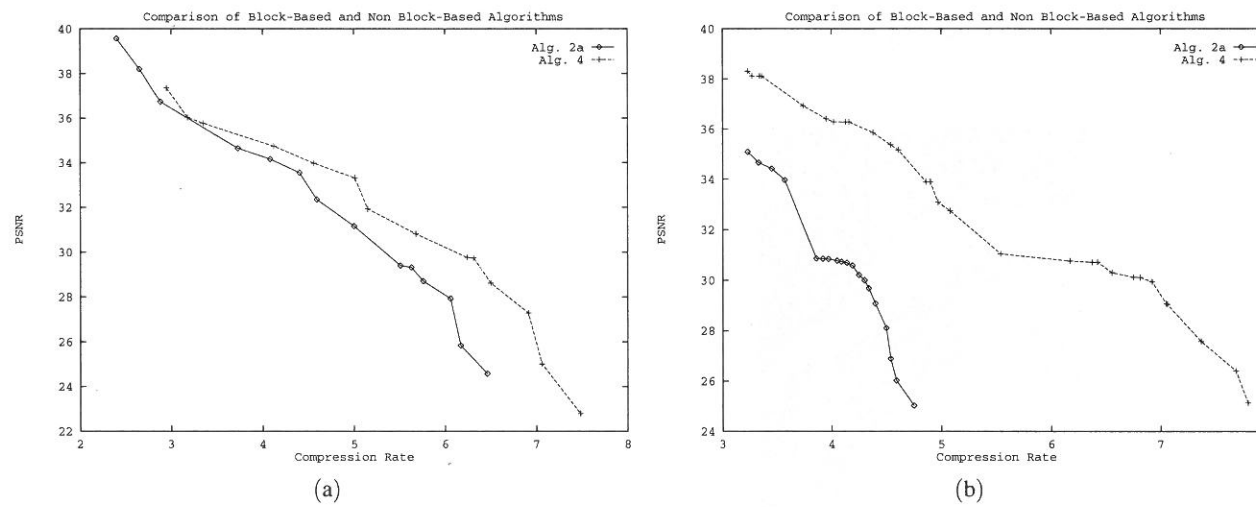

Fig. 9. Comparison of rate/distortion performance of Algorithms 2a and 4 with one large RoIs (see Figure 5.a) (a) and two smaller RoIs (see Figure 2) (b).

performance of algorithm 4 is clearly exhibited in both cases. Moreover, it is evident that the gap between block-based and generic approaches is much larger in the case of two RoIs. The obvious reason is that the amount of side information does not change for the generic algorithm whether one or more RoIs are considered, whereas the opposite is true for the block-based algorithm. The better results of the generic approach are confirmed when performing a visual comparison – the images in Figure 10 (RoI as given in Figure 5.a) are compressed with a rate of sligthly more than 6 and correspond to image quality of 25.5dB (Algorithm 2a - Figure 10.a) and 30.5dB (Algorithm 4 - Figure 10.b). As it is commonly known, it is problematic to judge image quality using "objective" numerical quality measures. In our case, numerical results and visual inspection confirm the same trend: the visible differences are as high as would have been expected from the numerical data (compare also Figures 5.b and 6). Figure 12 again shows a comparison of rate/distortion performance between Algorithms 2a and 4 (applied to the radiography in Figure 11). Whereas with Algorithm 4, we achieve compression rate 16 with acceptable quality (30.5 dB), Algorithm 2a already shows a much lower quality (27.5 dB) at compression rate 10. Additionally, in this case, Algorithm 2a is not even capable of achieving compression rates much higher than 10, regardless of the quality achieved.

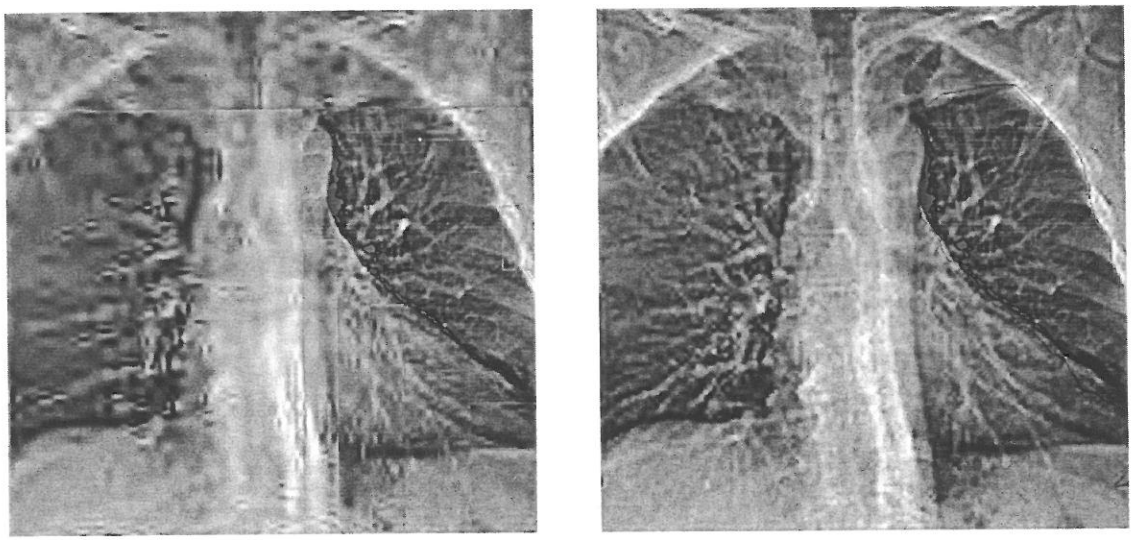

(a) (b)

Fig. 10. Visual quality of reconstructed images achieved by Algorithms 2a (a) and 4 (b) at compression rate 6 for RoI in Figure 5.a.

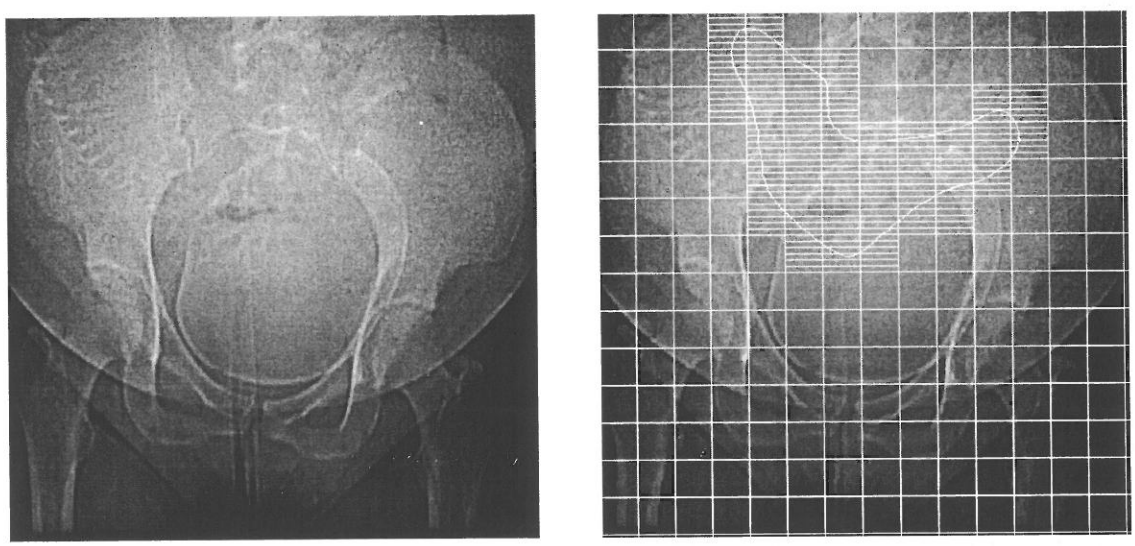

(a) (b)

Fig. 11. Original digital radiography (8bpp, 512 × 512 pixels) of a pregnant female (a) and corresponding RoI (b).

5. Conclusion

We observe that for a selective application of image compression a block-based wavelet compression approach is less suitable. Comparing generic approaches, the technique integrating the importance map and side information directly into the quantization and coding procedures turns out to be superior.

The demonstrated compression performance and the already known properties of common wavelet-based image compression, such as suitability for progressive transmission and low computational complexity make wavelet-based selective image compression an excellent choice for all types of telemedical and medical imaging applications.

Acknowledgements The authors thank Jutta

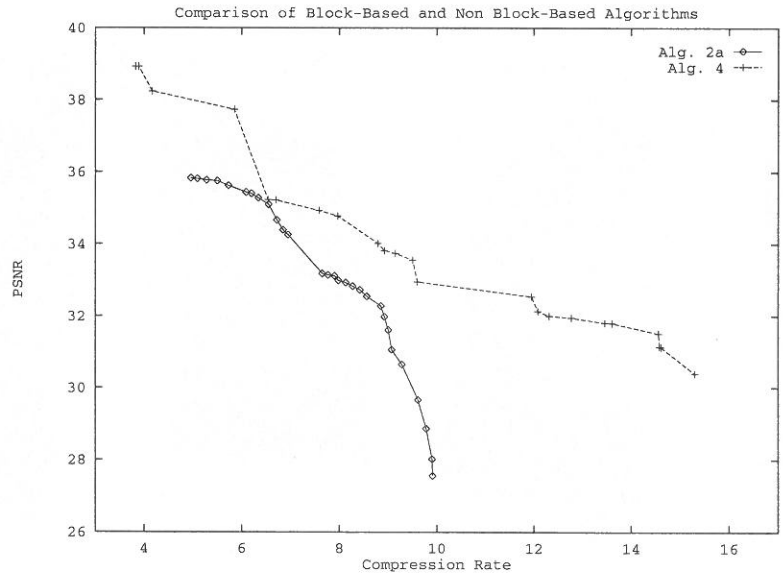

Fig. 12 Rate/distortion performance of Algorithms 2a and 4 for RoI in Figure 11.b.

Hämmerle for developing the graphical interface and Thomas Freina for implementing the bitplane-compression software.

References

[1] A. Aldroubi and M. Unser, editors. *Wavelets in Medicine and Biology*. CRC, Boca Raton, FL, 1996.

[2] M. Antonini, M. Barlaud, P. Mathieu, and I. Daubechies. Image coding using wavelet transform. *IEEE Transactions on Image Processing*, 1(2):205–220, 1992.

[3] A. Averbuch, D. Lazar, and M. Israeli. Image compression using wavelet transform and multiresolution decomposition. *IEEE Trans. on Image Process.*, 5(1):4–15, 1996.

[4] A.E. Cetin, O.N. Gerek, and S. Ulukus. Block wavelet transforms for image coding. *IEEE Transactions on Circuits and Systems for Video Technology*, 3(6):433–435, 1993.

[5] C.K. Chui, editor. *Wavelets: A Tutorial in Theory and Applications*. Academic Press, San Diego, 1992.

[6] A. Cohen, I. Daubechies, and P. Vial. Wavelets on the interval and fast wavelet transforms. *Appl. Comput. Harmon. Anal.*, 1(1):54–81, 1994.

[7] P.C. Cosman, R.M. Gray, and R.A. Olshen. Evaluating quality of compressed medical images: SNR, subjective rating, and diagnostic accuracy. *Proceedings of the IEEE*, 82(6):919–932, 1994.

[8] P.C. Cosman, R.M. Gray, and M. Vetterli. Vector quantization of image subbands: A review. *IEEE Transactions on Image Processing*, 5(2):202–225, 1996.

[9] I. Daubechies. Orthonormal bases of compactly supported wavelets. *Comm. Pure and Appl. Math.*, 41:909–996, 1988.

[10] P. Desarte, B. Macq, and D.T.M. Slock. Signal-adapted multiresolution transform for image coding. *IEEE Transactions on Information Theory*, 38(2):897–904, 1992.

[11] Y. Fisher, editor. *Fractal Image Compression: Theory and Application*. Springer-Verlag, New York, 1995.

[12] J. Froment and S. Mallat. Second generation compact image coding. In [5], pages 655–678. 1992.

[13] C. Herley, J. Kovacevic, K. Ramchandran, and M. Vetterli. Tilings of the time-frequency plane: Construction of arbitrary orthogonal bases and fast tiling algorithms. *IEEE Trans. on Signal Process.*, 12(41):3341–3359, 1993.

[14] M.L. Hilton, B.D. Jawerth, and A. Sengupta. Compressing still and moving images with wavelets. *Multimedia Systems*, 3(2), 1995.

[15] B.K.T. Ho, M.-J. Tsai, J. Wei, M. Ma, and P. Saipetch. Video compression of coronary angiograms based on discrete wavelet transform with block classification. *IEEE Transactions on Medical Imaging*, 15(6), December 1996.

[16] Y. Huh, J.J. Hwang, and K.R. Rao. Block wavelet transform coding of images using classified vector quantization. *IEEE Trans. on Circ. and Syst. for Video Tech.*, 5(1):63–67, 1995.

[17] B.D. Jawerth, M.L. Hilton, and T.L. Huntsberger. Local enhancement of compressed images. *Journ. Math. Imaging and Vision*, 1(3):39–50, 1993.

[18] G.R. Kuduvalli and R.M. Rangayyan. Performance analysis of reversible image compression techniques for high-resolution digital teleradiology. *IEEE Trans. on Medical Imaging*, 11(3):430–445, 1992.

[19] J. Lu, V.R. Algazi, and R.R. Estes. Comparative study of wavelet image coders. *Optical Engineering*, 35(9):2605–2619, 1996.

[20] S. Mallat. A theory for multiresolution signal decomposition: The wavelet representation. *IEEE Trans. on Patt. Anal. and Mach. Intell.*, 11(7):674–693, 1989.

[21] Y. Meyer. Ondelettes sur l'intervalle. *Revista Mat. Iberoamericana*, 7(2), 1991.

[22] Y.W. Nijim, S.D. Stearns, and W.B. Mikhael. Differentiation applied to lossless compression of medical images. *IEEE Trans. on Medical Imaging*, 15(4):555–559, 1996.

[23] L.P. Panych. Theoretical comparison of Fourier and Wavelet encoding in Magnetic Resonance Imaging. *IEEE Trans. on Medical Imaging*, 15(2):141–153, 1997.

[24] K. Ramchandran, M. Vetterli, and C. Herley. Wavelets, subband coding, and best bases. *Proceedings of the IEEE*, 84(4):541–560, 1996.

[25] A. Said and W.A. Pearlman. A new, fast, and efficient image codec based on set partitioning in hierarchical trees. *IEEE Transactions on Circuits and Systems for Video Technology*, 6(3):243–249, 1996.

[26] J.M. Shapiro. Embedded image coding using zerotrees of wavelet coefficients. *IEEE Trans. on Signal Process.*, 41(12):3445–3462, 1993.

[27] L. Shen and R.M. Rangayyan. A segmentation-based lossless image coding method for high resolution medical image compression. *IEEE Trans. on Medical Imaging*, 16(3):301–307, 1997.

[28] G. Sheppard. Selective Image Compression SLIC. Master's thesis, Southern College of Technology, Marietta, GA, 1994.

[29] T. Sikora. The MPEG-4 video standard verification model. *IEEE Transactions on Circuits and Systems for Video Technology*, 7(1):19–31, 1997.

[30] R.N. Strickland and H.I. Hahn. Wavelet transforms for detecting microcalcifications in mammograms. *IEEE Transactions on Medical Imaging*, 15(2):218–228, 1997.

[31] C. Taswell and K.C. McGill. Wavelet transform algorithms for finite-duration discrete-time signals. *ACM Transactions on Mathematical Software*, 20(3):398–412, 1994.

[32] A. Uhl. Adaptive wavelet image block coding. In H.H. Szu, editor, *Wavelet Applications III*, volume 2762 of *SPIE Proceedings*, pages 127–135, Orlando, FL, April 1996.

[33] A. Uhl. Image compression using non-stationary and inhomogeneous multiresolution analyses. *Image and Vision Computing*, 14(5):365–371, 1996.

[34] A. Uhl. Generalized wavelet decompositions in image compression: arbitrary subbands and parallel algorithms. *Optical Engineering*, 36(5):1480–1487, 1997.

[35] M. Unser and A. Aldroubi. A review of wavelets in biomedical applications. *Proceedings of the IEEE*, 84(4):626–638, 1996.

[36] I. Urriza, L.A. Barragan, J.I. Artigas, J.I. Garcia, and D. Navarro. Choice of word length in the design of a specialized hardware for lossless wavelet compression of medical images. *Optical Engineering*, 36(11):3033–3042, November 1997.

[37] J.D. Villasenor, B. Belzer, and J. Liao. Filter evaluation and selection in wavelet image compression. In J.A. Storer and M.A. Cohn, editors, *Proceedings Data Compression Conference DCC'94, Snowbird Utah*, pages 351–360. IEEE Computer Society, 1994.

[38] G.K. Wallace. The JPEG still picture compression standard. *Communications of the ACM*, 34(4):30–44, 1991.

[39] J. Wang and H.K. Huang. Medical image compression by using three-dimensional wavelet transformation. *IEEE Transactions on Medical Imaging*, 15(4), August 1996.

[40] S. Wong, L. Zaremba, D. Gooden, and H.K. Huang. Radiologic image compression – a review. *Proceedings of the IEEE*, 83(2):194–219, 1995.

[41] Z. Xiong, K. Ramchandran, and M.T. Orchard. Efficient arithmetic coding for wavelet image compression. In J. Biemond and E.J. Delp, editors, *Visual Communications and Image Processing '97*, volume 3024 of *SPIE Proceedings*, pages 13–24, San Jose, February 1997.

Received: June, 1997
Revised: April, 1998
Accepted: April, 1998

Contact address:
Alfred Bruckmann and Andreas Uhl
RIST++ (Research Institute for Softwaretechnology)
University of Salzburg

ALFRED BRUCKMANN received the B.S. and M.S. degrees (both in Mathematics) from the University of Salzburg. The presented work is part of his M.S. thesis. Currently he is Research Assistant at RIST++, University of Salzburg.

ANDREAS UHL received the B.S. and M.S. degrees (both in Mathematics) from the University of Salzburg and he completed his PhD on Applied Mathematics at the same University. He is currently faculty member at the Department of Computer Science and System Analysis and at the Research Institute for Softwaretechnology. His research interests include wavelets, image processing (with emphasis on image and video compression), numbertheoretical methods in numerical analysis, and parallel processing.